Measuring Melittin Uptake into Hydrogel Nanoparticles with Near Infrared Single Nanoparticle Surface Plasmon Resonance Microscopy

Kyunghee Cho, Jennifer B. Fasoli, Keiichi Yoshimatsu, Kenneth J. Shea, and Robert M. Corn*

Department of Chemistry, University of California, Irvine, Irvine, CA 92697, United States

Table of Contents

I. Optical Setup of the SPR Microscope

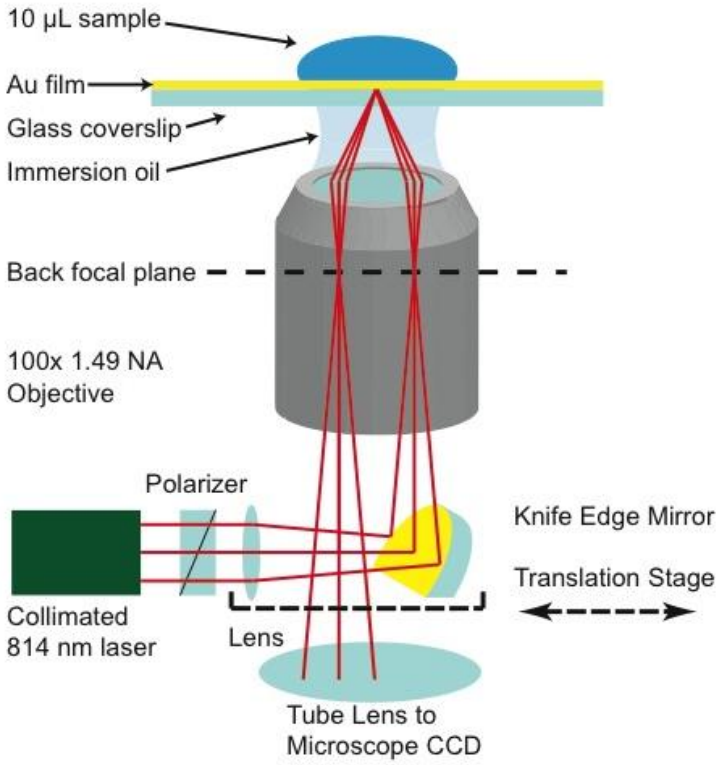

Figure S-1. Optical setup of the SPR microscope. A 1 mW 814 nm diode laser beam was polarized and focused with a lens (f = 200 mm) onto the back focal plane of a 100x 1.49 NA oil objective. The focused beam was directed up to the objective using a gold-coated knife-edge mirror attached to a translation stage to control the angle of incidence. The reflected image was passed to a CMOS camera.

II. DLS Analysis of Synthesized Hydrogel Nanoparticles

The mean hydrodynamic diameter of the hydrogel nanoparticles (HNPs) as measured by dynamic light scattering (DLS, measured by Zetasizer Nano ZS at 25 °C) was 220 nm in PBS. As detailed in the main text, the monomer feed ratios of the HNPs were 5 mol% AAc, 40 mol% TBAm, 2 mol% BIS, 53 mol% NIPAm. 2.5 mg/50 mL of SDS was used for the synthesis. The HNP synthesis yield was 89%

III. d*n*/d*c* and MALS Measurements to Determine Mean HNP Molar Mass

To determine the refractive index increment (d*n*/d*c*) value of hydrogel particles, differential refractive indexes of aqueous solutions containing 15.6, 31.3, 62.5, 125, 250, and 500 µg/mL of hydrogel particles were measured by using Optilab rEX equipped with a syringe pump. Multi-angle light scattering (MALS) of aqueous solutions containing 1.60, 2.40, 3.60, 5.40, 7.20, 9.60, and 12.8 µg/mL of hydrogel particles were measured by using DAWN HELEOS equipped with a syringe pump. Both differential refractive index and multi-angle light scattering measurements were performed under a flow condition (0.38 mL min^{-1}). Data collection and subsequent data analysis were performed by using the Astra software Version 5.3.4.20 (Wyatt Technology Corporation, Santa Barbara, CA). The principles employed in multi-angle light scattering date analysis have been described in detail elsewhere.[1]

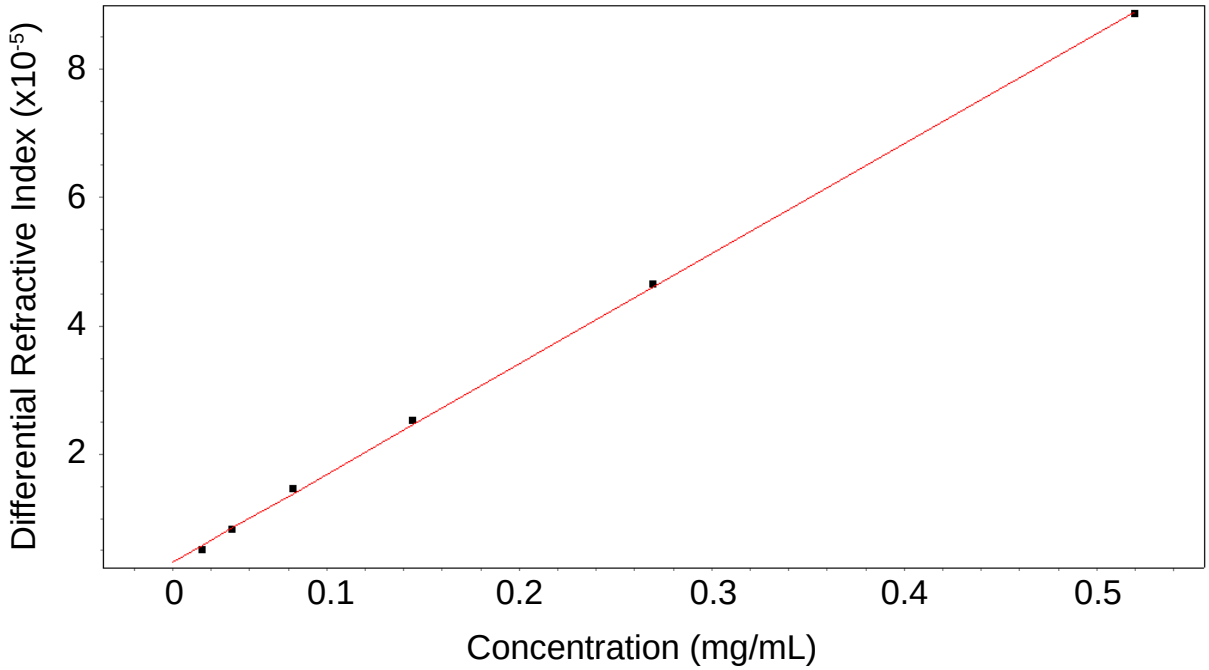

Figure S-2. d*n*/d*c* determination from differential refractive index measurements.

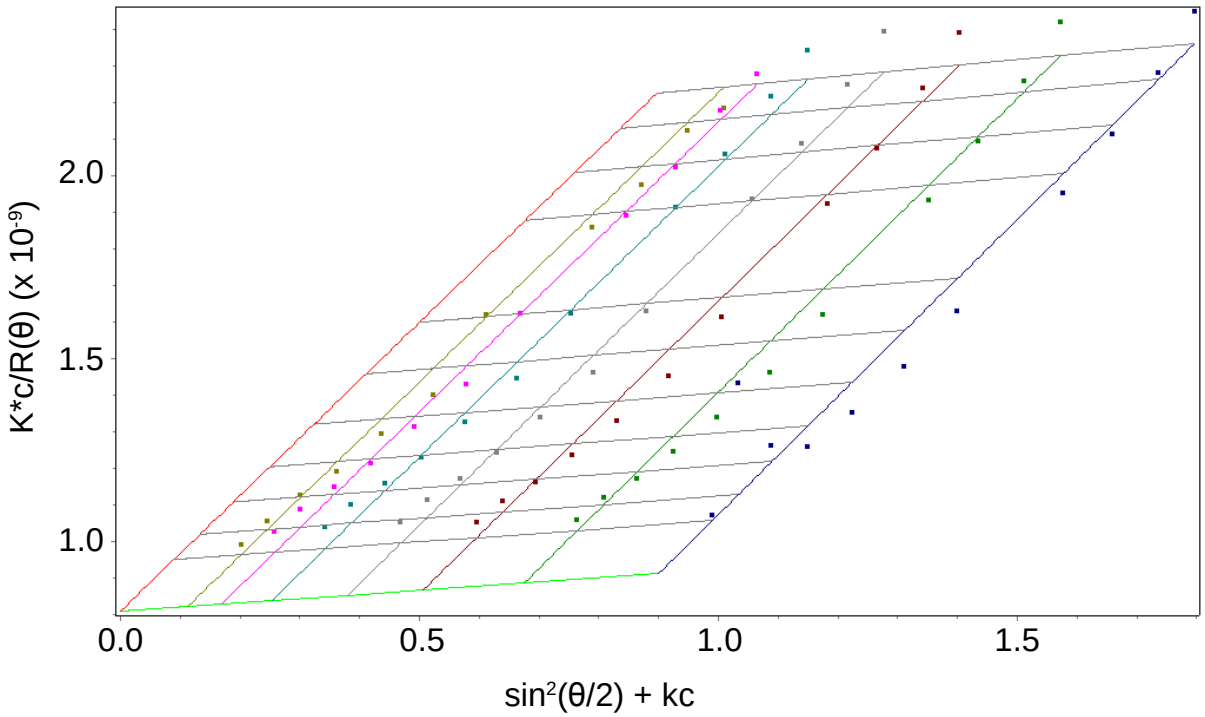

Figure S-3. Zimm plot generated from HNP concentrations noted above.

Results of static light scattering experiments:

Refractive index increment (d*n*/d*c*): 0.1714 ± 0.0016 mL g^{-1}

Radius of gyration (R_g): 95.2 ± 2.0 nm

Second Virial Coefficient (A_2): (4.020 ± 1.756) × 10^{-6} mol mL g^{-2}

Molar mass (MW): (1.235 ± 0.038) × 10^{9} g mol^{-1}

IV. Average Single Nanoparticle SPRM Reflectivity Change $<\Delta\%R_{NP}>$

Table S-1. SPRM response to melittin loading.

Melittin concentration (μM)	$<\Delta\%R_{NP}>$	Standard deviation (Δ%R)	95% Confidence interval (Δ%R)	N
0	1.04	0.30	0.03	443
0.5	1.19	0.52	0.06	314
1.0	1.44	0.50	0.06	304
1.5	1.61	0.52	0.06	300
2.0	1.80	0.41	0.04	392
2.5	2.10	0.50	0.05	355

V. Fluorescence Measurements

The intrinsic fluorescence of melittin due to its sole tryptophan residue has been documented previously.[2,3] Samples were excited at 280 nm and their fluorescence emission measured at 349 nm. Measured fluorescence values were converted to concentration from standard curves generated from melittin solutions of varying concentrations in PBS.

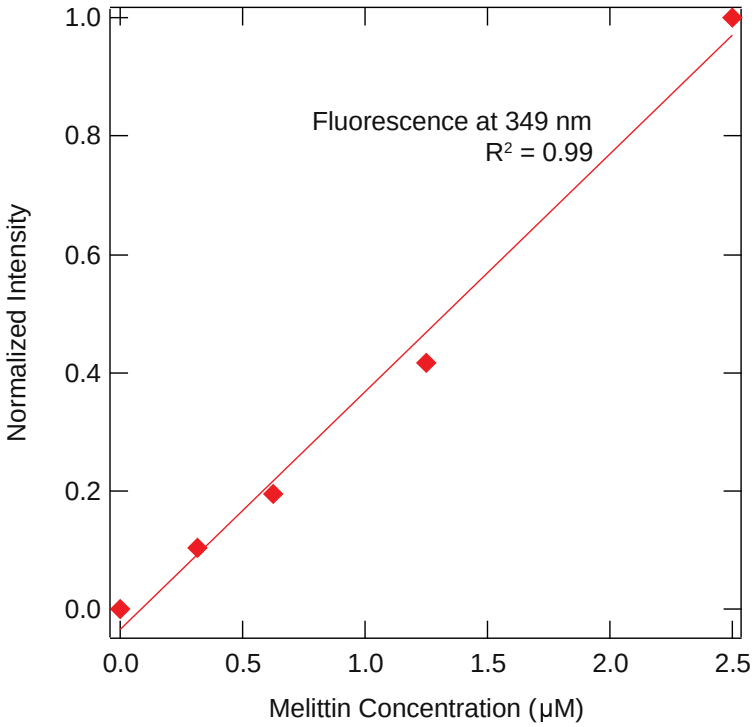

Figure S-4. Melittin fluorescence standard curve for measured emission at 349 nm.

Table S-2. Fluorescence Characterization of Melittin Uptake by HNPs

Concentration (μM)	Concentration Measured by Fluorescence (μM)		Melittin Absorbed by HNPs (%)	Melittin Molecules/HNP
	With HNPs	Without HNPs		
0	0.05 ± 0.08	0.05 ± 0.09	n/a	n/a
0.5	0.18 ± 0.01	0.46 ± 0.06	62	10,000
1	0.27 ± 0.03	0.72 ± 0.08	63	21,000
1.5	0.46 ± 0.01	1.60 ± 0.05	71	36,000
2	0.42 ± 0.02	2.14 ± 0.13	80	53,000
2.5	0.54 ± 0.06	2.48 ± 0.33	78	65,000

The moles of melittin (from the initial concentration and the percentage of melittin absorbed as measured by fluorescence) and moles of HNPs (from 30 pM) in the ultracentrifuged volume of 5 mL were first calculated (e.g., at 2.5 μM melittin, 78% of melittin was absorbed by HNPs; 0.78 x 2.5 μM x 5 mL = 9.75 nmol melittin; 30 pM HNPs x 5 mL = 150 fmol HNP). Their molar ratio is the estimated melittin molecules/HNP that is reported.

VI. HNP Aggregation at High Melittin Concentrations Observed by SPRM

For melittin concentrations up to 2.5 μM, we see a linear increase in $<\Delta\%R_{NP}>$ proportional to peptide concentration. When HNPs are mixed into higher concentrations of melittin, we see evidence of HNP aggregation in very large diffraction features with large $\Delta\%R_{NP}$ values ($\Delta\%R_{NP} > 4\%$). This aggregation is likely the due to charge neutralization of the HNPs by melittin. As a result of these aggregates, the standard deviation of the $\Delta\%R_{NP}$ distribution increases significantly. For example, a solution of 5.4 μM melittin and 30 pM HNPs results in a $\Delta\%R_{NP}$ distribution with a standard deviation of 1%, as seen in Figure S-5. This observation is corroborated by DLS, which also detects the presence of aggregates, but analysis by SPRM gives deeper insight into the nature of this aggregation. For example, for the 5.4 μM melittin solution mentioned above, roughly 6% of the signal observed were greater than 4% in

$\Delta\%R_{NP}$ and deemed as aggregates. We are also able to visualize and track in real time the formation of HNP aggregates as they adsorb onto the surface.

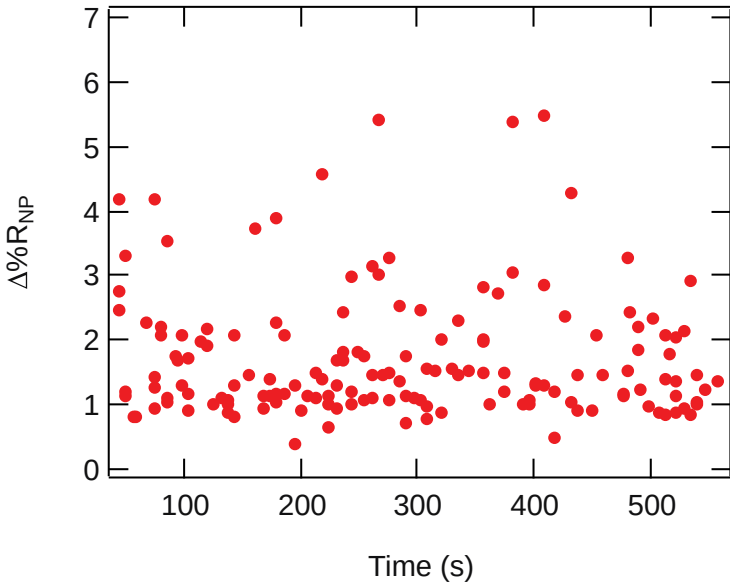

Figure S-5. $\Delta\%R_{NP}$ distributions over time for a solution containing 5.4 μM melittin and 30 pM HNPs in PBS. HNP aggregates appeared as very large signals ($\Delta\%R_{NP}$ > 4%) and made up ~6% of the all $\Delta\%R_{NP}$ calculated. The standard deviation of the $\Delta\%R_{NP}$ distribution increased to 1% for this experiment, which is much larger than without HNP aggregation. HNP aggregation was also detected by DLS.

Supporting Information References:

(1) Andersson, M.; Wittgren, B.; Wahlund, K.-G. *Anal. Chem.* **2003**, *75*, 4279.

(2) Raghuraman, H.; Chattopadhyay, A. *Biophys. J.* **2004**, *87*, 2419–2432.

(3) Tran, C.D.; Beddard, G.S. *Eur. Biophys. J.* **1985**, *13*, 59-64.